Metabolism of Dynorphin A 1-13 in Human Blood and Plasma

Stefan Müller[1] and Günther Hochhaus[1,2]

Received July 27, 1994; accepted February 21, 1995

Purpose. A detailed investigation of the metabolic routes and rates of Dyn A1-13 in human blood and plasma was performed. ***Methods.*** Human plasma was incubated at 37°C with dynorphin A 1-13 (Dyn A1-13, 15-20 μM). The generated dynorphin fragments were separated by a new ion-pair chromatographic method and identified by matrix assisted laser desorption mass spectroscopy. The kinetic behavior of parent compound and metabolites was evaluated in the absence and presence of enzyme inhibitors. ***Results.*** The major plasma metabolites of Dyn A1-13 were Dyn A1-12, A2-12, A4-12 and A4-8. Further metabolites were Dyn A2-13, A3-13, A3-12, A5-12, A6-12, A7-12, A1-10, A2-10, A2-8 and A3-8. At 37°C, Dyn A1-13 had a half-life of less than one minute in plasma and blood. Plasma half-lives of major metabolites ranged between 0.5 and 4 min. Inter- and intra-individual differences in healthy volunteers were 30% (c.v.). Dyn A1-13 is mainly metabolized by carboxypeptidases to Dyn A1-12 (80%) and by aminopeptidases to Dyn A2-13 (15%). Dyn A1-12 and Dyn A2-13 are predominantly converted into Dyn A2-12 (67% of Dyn A1-13). Subsequent metabolic steps yield Dyn A3-12 (16%), Dyn A4-12 (37%) and Dyn A4-8 (33%). Aminopeptidases generate Dyn A2-12, A3-12, A4-12, A5-12. ACE metabolizes Dyn A1-12 (19%), A2-12 (33%), A3-12 (34%) and A4-12 (46%). Bestatin-sensitive endopeptidases (possibly endopeptidase 24.11) metabolize 30% of Dyn A2-12. Dyn A4-8 is formed via Dyn A4-12 (23% of Dyn A4-12) and Dyn A2-10 (37% of Dyn A2-10). ***Conclusions.*** The combination of enzyme inhibition experiments and noncompartmental kinetic analysis proved to be a powerful tool for the detailed evaluation of the metabolic fate of Dyn A1-13 in human blood and plasma.

KEY WORDS: dynorphin A1-13; opioid peptides; metabolism; pharmacokinetics; HPLC.

INTRODUCTION

Dynorphin A 1-13 (Dyn A1-13, YGGFLRRIRPKLK) is a potent opioid peptide (1). It has been shown to modulate pain, tolerance and addiction and has shown to attenuate the effects of opiate withdrawal (2-4). Knowledge about its metabolic fate is very limited. Leslie and Goldstein (5) investigated the metabolism of Dyn A1-13 in rat brain membranes. Very recently, some metabolites of Dyn A1-13 in blood have been reported as Dyn A1-12, A1-6, A1-12 and A3-12 (6) without further kinetic characterization.

The objective of this study was to obtain detailed information on the metabolic routes and rates of Dyn A1-13 and its metabolites in human plasma and blood as potential metabolic sites for intravenously given Dyn A1-13. Relevant Dyn A1-13 processing peptidases in plasma were identified and their relative importance in the overall metabolism assessed by in-vitro pharmacokinetic and enzyme inhibition studies. This lead to a detailed understanding of the metabolic fate of Dyn A1-13, up to the 5th metabolic generation, and an estimation of variability among healthy volunteers. The developed strategies are applicable to the detailed assessment of the metabolic fate of other peptide drugs.

[1] Department of Pharmaceutics, JHMHC Box 100494, University of Florida, Gainesville, Florida 32610.

[2] To whom correspondence should be addressed.

MATERIALS AND METHODS

Materials

Dyn A2-12, A3-12, A4-12, A2-11, A2-10, A2-8 and A4-8 were custom synthesized by the Protein Chemistry Core Facility, Interdisciplinary Center for Biotechnology Research, University of Florida. All other peptides were obtained from commercial sources with purities indicated by the manufacturer. Bestatin, captopril, L-leucinethiol (oxidized), N-ethylmaleimide, thiorphan was obtained from Sigma (St. Louis, MO), (2-Guanidinoethylmercapto) succinic acid (GEMSA) from Fluka (Buchs, Switzerland), and difluorophosphate (DFP) from Aldrich (Milwaukee, WI). All other chemicals were of analytical or HPLC grade.

Sample Preparation

Blood was collected from the arm vein of 6 Caucasian, healthy, male volunteers (age 25-30) and transferred into heparinized polypropylene centrifuge tubes. Plasma was used immediately or stored at −60°C, as freezing did not change enzymatic activity.

The following inhibitors were suitable to fully block the indicated enzymes: Bestatin (300 μM, aminopeptidases), L-leucinethiol, oxidized (8.5 μM, aminopeptidases), DFP (1 mM, dipeptidyl-aminopeptidase), thiorphan (15 μM, endopeptidase 24.11), captopril (100 μM, angiotensin converting enzyme, ACE) and GEMSA (10 μM, carboxypeptidase N). Five minutes after addition of inhibitors (if applicable), peptides (50 μg, net weight) were added to 1 ml of plasma or blood. 100 μl aliquots were removed at defined time points and transferred into 100 μl of a blocking solution (5 vol of a 5% aqueous $ZnSO_4$ solution, 3 vol of acetonitrile, 2 vol of methanol). After centrifugation (10,000 g, 2.5 min), 100 μl of clear supernatant was stored on ice until analyzed. Dyn A1-13 was stable in plasma pretreated with blocking solution over a time period of 24 hours.

Chromatography

Mobile phase A consisted of 10% acetonitrile in aqueous trifluoroacetic acid (TFA, 0.03%V/V) containing 30 mM pentanesulfonic acid sodium salt (PSA). Mobile phase B consisted of 90% acetonitrile in aqueous TFA (0.03%V/V) and 30 mM PSA. Separation system I consisted of a 10 μm Waters C-18 reversed phase column using a 30 min linear gradient of 20 to 40% mobile phase B. Separation system I without PSA was used to demonstrate the advantages of ion pair chromatography (see Fig. 1). Separation system II was used for the elucidation of Dyn A1-12, A2-12 and A3-12 metabolism. It consisted of a 5μm Spherisorb ODS 2 column (Keystone Scientific) and a 30 min linear gradient from 25 to 45% mo-

0724-8741/95/0800-1165$07.50/0

bile phase B. Calibration curves were established in a mixture of plasma and blocking solution and corrected for peptide purity. r^2 Values were larger than 0.997.

Metabolite Purification for Mass Spectroscopy

Plasma spiked with Dyn A1-13 (100 μM) was incubated at 37°C for 30 min. After addition of blocking buffer and centrifugation at 10,000 g for 5 min, 100 μl clear supernatant was injected into HPLC system I. Identical controls with blank plasma were checked for potential interferences by endogenous substances.

HPLC-fractions were collected, concentrated and applied to activated Supelclean LC-18 SPE cartridges, washed with 2 ml of 3% aqueous acetic acid and eluted with 500 μl of methanol in 3% aqueous acetic acid (70%V/V). The eluent was subjected to mass spectroscopy.

Mass Spectrometry (MS)

Matrix assisted laser desorption mass spectrometry (LD-MS) was performed on a Vestec LaserTec instrument by the Protein Chemistry Core Facility (Center for Biotechnology Research, University of Florida).

Data Analysis

Concentration-time profiles of parent compounds and metabolites were analyzed by RSTRIP (Micromath, UT) assuming pseudo-first order metabolic processes. Half-lives of appearance or disappearance were calculated from the corresponding rate (k) as 0.693/k. The area under the concentration-time profiles were calculated by the trapezoidal rule. Areas after the last measurement point (Cp_x) were estimated from Cp_x/k, with k describing the terminal slope of concentration time profiles.

The conversion of a peptide into a specific metabolite (F_{AUC}) was calculated from the AUC of the metabolite (AUC_{met})

$$AUC_{met}/AUC_{100\%} *100 = F_{AUC} \quad (1)$$

Therefore, the AUC of full conversion ($AUC_{100\%}$) was calculated from the molar concentration of the parent compound at t = 0 (Cp_0) and the degradation rate k_{deg} of the metabolite: $AUC_{100\%} = Cp_0/k_{deg}$.

The fraction F_{EnzInh}, describing the participation of a specific enzyme on the overall metabolism was calculated from the half-lives of a given peptide in the presence ($t_{0.5inh}$) or absence ($t_{0.5deg}$) of enzyme inhibitor:

$$F_{EnzInh} = (1 - t_{0.5deg}/t_{0.5inh})*100$$

Parent-compound and first metabolite concentration-time profiles were also fitted simultaneously to first order kinetics using Scientist (Micromath, UT) and standard pharmacokinetic relationships.

RESULTS

Gradient reversed phase HPLC with PSA as ion pairing reagent (system I) allowed the separation of dynorphin fragments (Dyn A1-13 and A2-12) not resolved under non-ion pairing conditions (Figure 1). Coelution of Dyn A2-12 and Dyn A3-12 in system I lead to the development of system II (Figure 1).

Incubation of Dyn A1-13 yielded a number of metabolites which were resolved on HPLC system I (Figure 2). Five fractions containing each one major and multiple smaller peaks (Figure 2) were analyzed by LD-MS. The resulting molecular weights are listed in Table I. The identity of major metabolites was further proven by comparing its HPLC retention behavior with custom-synthesized fragments (Table I). The main metabolites were determined to be Dyn A1-12, A2-12, A4-12 and A4-8. Additional metabolites were Dyn

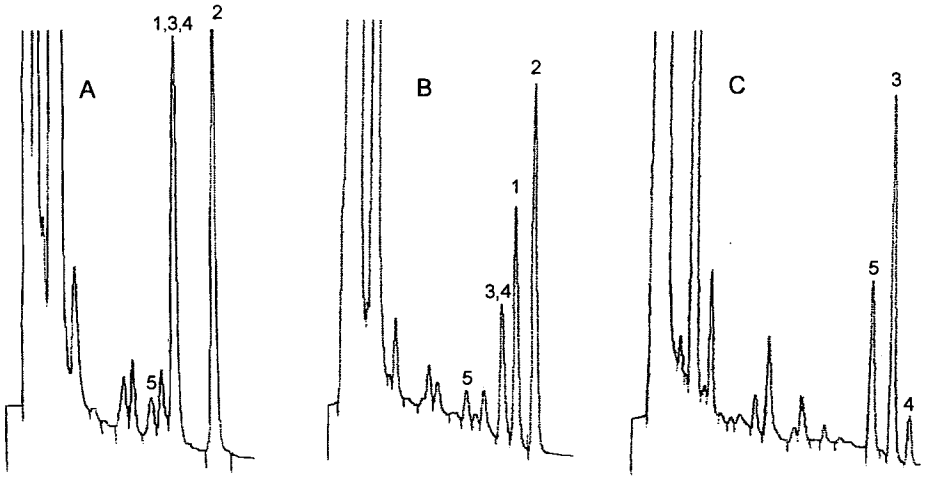

Fig. 1. Separation of Dyn A 1-13 and metabolites by gradient reversed phase chromatography without (A) and with pentane sulfonic acid as ion pairing reagent (B: separation system I, C: separation system II): Chromatogram A demonstrates that Dyn A 1-13 (1) is not resolved from Dyn A 2-12 (3) or Dyn A 3-12 (4) under non-ion pairing conditions. Dyn A2-12 (3) coelutes in chromatogram B with Dyn A 3-12 (4). Chromatogram C shows further separation of Dyn A 3-12 (4) from Dyn A 2-12 (3) in separation system II in the absence of Dyn A 1-12 and Dyn A 1-13. Dyn A 1-12 (2) and Dyn A 4-12 (5) were well resolved under all conditions not shown in C. Chromatograms represent spiked plasma samples.

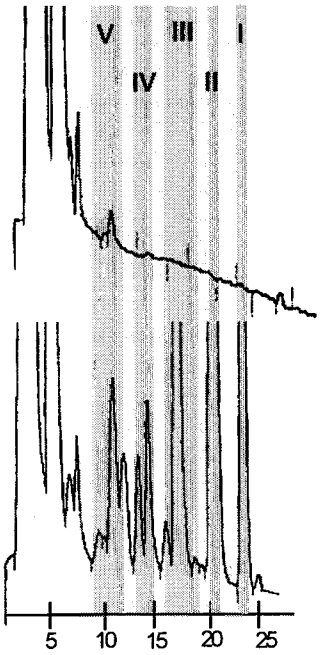

Fig. 2. Collection of metabolites for LD-MS: Plasma was spiked with Dyn A 1-13, the enzymatic reaction stopped by adding blocking solution (cp. methods section, sample preparation). HPLC fractions corresponding to the shaded areas (I-V) were collected and further processed for LD-MS.

A2-13, A3-13, A3-12, A5-12, A6-12, A7-12, A1-10, A2-10, A2-8 and A3-8. Analysis of blank plasma samples revealed no interference with endogenous substances.

The time profiles of direct degradation of Dyn A1-13 and its main metabolites in plasma (Figure 3) and blood (not shown) followed first order kinetics for parent compounds and first metabolites ($r^2 > 0.99$). When Dyn A1-13 and metabolites were directly incubated in the plasma, degradation half-lives, obtained from least square fits ($r^2 > 0.994$) ranged from 0.5 to 4 min (Table II).

F_{AUC}-data (Tables III and IV) revealed that, 78% of Dyn A1-13 is transformed into Dyn A1-12, while 15% are entering the Dyn A2-13 pool. Further degradation leads to Dyn A2-12 (67%), A3-12 (16%), A4-12 (37%) and A4-8 (3%). 23% of Dyn A4-12 but 33% of Dyn A1-13 was converted into Dyn A4-8. Other minor metabolites (e.g. Dyn A1-10 and A2-8) contributed to the formation of Dyn A4-8 (Table IV).

Intra-individual variability in plasma of one volunteer was generally smaller than 30% when half-lives and pool sizes of major metabolites were compared for Dyn A1-13 and A1-12 (Table III). Similar values were obtained for the inter-individual variability (Table III). No significant differences between plasma and blood were detected (Table III).

Enzyme inhibition studies were carried out to identify the enzymes involved in the metabolism of Dyn A1-13 (Table V). The carboxypeptidase inhibitor GEMSA increased $t_{1/2}$ of Dyn A1-13 (Table II) indicating that 82% of Dyn A1-13 enters the Dyn A1-12 pool (Table V).

Aminopeptidases were also involved in the metabolism of Dyn A1-12 into Dyn A2-12 (Table V). A dissociation of the effects of bestatin and leucinethiol on the metabolism of Dyn A2-12 occurred (Table V). While the formation of Dyn A3-12 and Dyn A4-12 was blocked by bestatin, leucinethiol inhibited the formation of Dyn A3-12 but not of Dyn A4-12. Dyn A4-12 was affected by ACE (captopril) as well as aminopeptidase (leucinethiol) inhibitors (Table II and V). Dyn A2-12 and Dyn A4-12 was not affected by DFP (dipeptidyl-aminopeptidase inhibitor). Thiorphan (enkephalinase A inhibitor) did not alter Dyn A1-12, but Dyn A2-12 metabolism

Table I. Identification of Metabolites by LD-MS and HPLC: Molecular Weights of Dynorphin Fragments Identified in Peaks of Figure 2 are Shown Together with Possible Sequences. HPLC Retention Times of Metabolites and Custom Synthesized Dynorphin Fragments Were Compared Whenever Possible

HPLC-fraction (retention time window)	Mol. weight of found fragments(s)	Possible Dyn A1–13 fragment sequence (nominal mol. weight)	Coelution with synthesized fragment
I (23 min)	1477[a]	Dyn A1–12 (1477)	Yes
II (20 min)	1604[a]	Dyn A1–13 (1604)	Yes
III (18–19 min)	1256	Dyn A3–12 (1253)	Yes
	1384	Dyn A3–13 (1384)	Not tested
	1314[a]	Dyn A2–12 (1313)	Yes
	1235	Dyn A1–10 (1234)	Not tested
IV (13–17 min)	1441	Dyn A2–13 (1441)	Yes
	1199[a]	Dyn A4–12 (1199)	Yes
		Dyn A2–11 (1200)	No
	1051	Dyn A5–12 (1051)	Not tested
	1072	Dyn A2–10 (1071)	Not tested
	818	Dyn A2–8 (818)	Not tested
	762	Dyn A3–8 (761)	Not tested
V (9–11 min)	938	Dyn A6–12 (938)	Not tested
	782	Dyn A7–12 (782)	Not tested
	957	Dyn A4–10 (957)	Not tested
	704[a]	Dyn A4–8 (704)	Yes
		Dyn A2–7 (705)	Not tested

[a] Major peaks in LD-MS spectra.

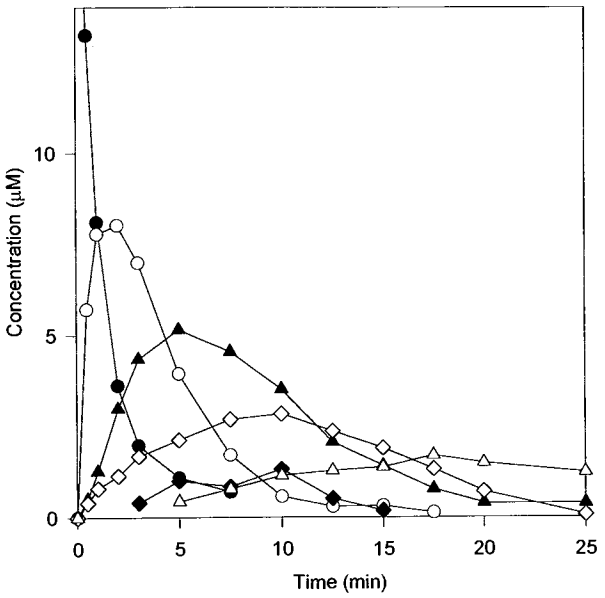

Fig. 3. Concentration-time profiles of Dyn A 1-13 (●) and major metabolites (Dyn A 1-12 ○, Dyn A 2-12 ▲, Dyn A 3-12 ◆, Dyn A 4-12 ◇ and Dyn A 4-8 △) in human plasma at 37°C.

(Table II). Most of the Dyn A4-12 metabolism was bestatin sensitive, indicating a predominant conversion into Dyn A5-12. Figure 4 depicts the main metabolic pathways of Dyn A1-13 based on Table IV and V.

DISCUSSION

Dyn A1-12, A2-12, A3-12 and A4-12 have also been found in whole blood by HPLC-MS (6). In addition, our study revealed the formation of Dyn A3-13, A5-12, A6-12, A7-12, A1-10, A2-10, A2-8, A3-8 and A4-8, some of which have been shown pharmacologically active in animal models (3). We failed, however, to identify Dyn A1-6 as a major metabolite (6). This is supported by enzyme inhibition studies (Table II and V) as 91% of Dyn A1-13 in blood and plasma is metabolized via exopeptidases. Dyn A1-6 can therefore only represent a minor metabolite.

While Chou and co-workers (6) reported four of the main metabolites while developing a new MS method, we were mainly interested in an in-vitro pharmacokinetic evaluation of the metabolic fate of Dyn A1-13 in human plasma and blood with the final goal of identifying the detailed metabolic pathways of Dyn A1-13, as a model for the development of general strategies for the detailed assessment of plasma peptide metabolism.

No differences in the metabolic profiles were found between blood and plasma (Table III) supporting the notion that plasma may be sufficient as an in vitro predictor for the in vitro metabolism in blood (7).

Analysis of concentration-time profiles of parent drugs and first metabolite generation, even in the presence of enzyme inhibitors did not reveal any deviation from first order processes. Hence, primary and secondary metabolic pathways showed first order characteristics. This justified the mathematical models employed.

The inter-individual variability among the rather homogenous group was small (Table III) and not different from those generally observed in pharmacokinetic studies. Thus, no major problems in designing reproducible blood levels are anticipated. The rather short half-lives assessed for intact drug and metabolites will be a challenge for an convenient and cost-effective dosing.

The main metabolite of Dyn A1-13 was Dyn A1-12 (80%, Figure V). The responsible enzyme was identified as carboxypeptidase N. It is known to cleave preferentially peptides with basic C-terminal amino acids such as lysine (8). The distinct increase of Dyn A1-13 stability under GEMSA inhibition further confirmed its participation in the metabolism of Dyn A1-13.

Enzyme inhibition studies and MS data suggested also Dyn A2-13 as a minor Dyn A1-13 metabolite. Dyn A1-13 incubation under carboxypeptidase inhibition (GEMSA) revealed its appearance with a half-life of formation of 4.5 min

Table II. Half-Lives of Dynorphin Fragments in Plasma with and Without Enzyme Inhibition

Peptide incubated	n	Half-life ± SD (min)	Main metabolite	Half-lives under inhibition (min)				
				GEMSA	Captopril	Bestatin	Leucinethiol	DFP
Dyn A1-13	3	0.9 ± 0.1	Dyn A1-12	4.4	N.T.	1.25	0.8	N.T.
Dyn A2-13	1	0.7	Dyn A2-12	N.T.	N.T.	N.T.	N.T.	N.T.
Dyn A1-12	3	1.9 ± 0.1	Dyn A2-12	N.T.	2.4	15.4	10.9	N.T.
Dyn A2-12	4	3.2 ± 0.1	Dyn A4-12	2.6	4.8	16.7	5	2.4
Dyn A3-12	2	2.1/2.8	Dyn A4-12	N.T.	2.9	14	N.T.	N.T.
Dyn A4-12	3	4.1 ± 0.4	Dyn A5-12	N.T.	7.6	16.6	6.9	3.6
Dyn A1-10	2	1.3/1.5	Dyn A2-10	N.T.	N.T.	N.T.	N.T.	N.T.
Dyn A2-10	1	2.3	Dyn A4-10	N.T.	4.2	5.8	N.T.	N.T.
Dyn A1-8	1	0.7	unknown	N.T.	N.T.	N.T.	N.T.	N.T.
Dyn A2-8	2	2.6/2.5	Dyn A4-8	N.T.	7.1	4.5	N.T.	N.T.
Dyn A4-8	2	2.8/3.3	unknown	N.T.	N.T.	6.3	N.T.	N.T.
Dyn A1-6	1	0.75	unknown	N.T.	N.T.	N.T.	N.T.	N.T.

N.T. = not tested.

Half-lives of dynorphin fragments in untreated plasma and in the presence of enzyme inhibitors are listed. The use of relevant enzyme inhibitors resulted in prolonged half-lives. Enzyme inhibition data was used to identify peptidases involved in dynorphin metabolism and the assessment of their relative importance (F_{Enzinh} see Methods and Table IV).

Table III. Noncompartimental (AUC-Based) Comparison of Dyn A1–13 Metabolism in Full Blood and Plasma, Inter- and Intraindividual Differences in Plasma: No Significant Differences in the Metabolism in Full Blood and Plasma Can Be Detected. The Interindividual Differences Within the Sampled Population (White Caucasians, Age: 25–30 Years) Were No Different from the Intraindividual Differences

Half-lives ± SD (min)		Fraction of initial Dyn A1–13 converted into listed metabolite (in % ± c.v.)				
Dyn A1–13	Dyn A1–12	Dyn A1–12	Dyn A2–12	Dyn A3–12	Dyn A4–12	Dyn A4–8
Interindividual variability in full blood, n = 6						
0.85 ± 0.27	2.26 ± 0.40	81 ± 10	57 ± 13	19 ± 5	59 ± 20	30 ± 12
Interindividual variability in plasma, n = 6						
0.78 ± 0.10	2.37 ± 0.23	78 ± 9	67 ± 12	16 ± 3	37 ± 6	33 ± 9
Intraindividual variability in plasma, n = 4						
0.93 ± 0.14	1.81 ± 0.14	78 ± 7	66 ± 8[a]		34 ± 8	24 ± 22

[a] Data was obtained on separation system I, hence no resolution of Dyn A2–12 and Dyn A3–12.

(data not shown). This and the observation that under aminopeptidase inhibition an almost complete transformation into Dyn A1-12 occurred (94% for bestatin) demonstrates that mainly carboxypeptidases but to a lesser degree also aminopeptidase are responsible for the metabolism of Dyn A1-13.

The C-terminal leucine of Dyn A1-12 terminated appreciable carboxypeptidase activity. Enzyme inhibition and non-compartmental evaluation suggested a 80% conversion into Dyn A2-12, making aminopeptidase the major degrading enzyme of Dyn A1-12. A minor metabolic route is the formation of Dyn A1-10 via ACE as suggested by MS-data and the modulation of the half-life of Dyn A1-12 by captopril. We were, however, unable to follow this metabolite by HPLC, probably due to its comparably slow formation and rapid degradation (Dyn A1-10, Table II). A mixture of leucinethiol and captopril prolonged the half-life of Dyn A1-12 to over one hour, no formation of Dyn A4-12 was observed. Thiorphan (enkephalinase A inhibitor) failed to increase the half-life of Dyn A1-12 (Table V). Both experiments suggested that Dyn A 4-12 is not a direct metabolite of Dyn A1-12. Dyn A2-12 was not only generated via Dyn A1-12, but also via Dyn A2-13 (78% and 89% respectively, based on F_{AUC}, Table IV). Thus, the degradation of Dyn A1-13 up to the formation of Dyn A2-12 is dominated by carboxypeptidases and aminopeptidases and resembles the degradation of Dyn A1-13 by rat cranial membranes (5).

The next major metabolite detected downstream of Dyn A2-12 was Dyn A4-12 (37% of the initial Dyn A1-13). Analysis of Dyn A2-12 degradation revealed also the formation of Dyn A3-12 (Table IV). As only 16% was converted into Dyn A3-12, but 37% Dyn A4-12 was formed, Dyn A4-12 must be formed via two pathways. Thiorphan blocked 28% of the overall Dyn A2-12 metabolism. Thus, Dyn A2-12 seems to be metabolized N-terminally into Dyn A3-12 (16%) and into Dyn A4-12 (28%) by aminopeptidases and a thiorphan sensitive endopeptidase (Table IV and V). The discrepancy between the inhibition of bestatin and leucinethiol is in good agreement with recent reports on lacking bestatin specificity (9).

Table IV. Noncompartimental Kinetic (AUC-Based) Analysis of the Conversion of Dynorphin Fragments into Their Major Metabolites. For Details See Methods Section

Peptide incubated	n	Fraction of initial dynorphin fragment converted into listed metabolites (in % ± c.v. calculated as F_{AUC})						
		Dyn A1–13	Dyn A1–12	Dyn A2–13	Dyn A2–12	Dyn A3–12	Dyn A4–12	Dyn A4–8
Dyn A1–13	6	100	78 ± 9	15 ± 5	67 ± 12	16 ± 3	37 ± 6	33 ± 9
Dyn A1–12	1		100	—	78	18	59	23
Dyn A2–13	1			100	89*	—*	39	30
Dyn A2–12	3				100	17 ± 6	42 ± 20	30 ± 8
Dyn A3–12	1					100	73	23
Dyn A4–12	4						100	23 ± 7
						Dyn A1–10	Dyn A2–10	Dyn A4–8
Dyn A1–10	1					100	68	35
Dyn A2–10	1						100	37
						Dyn A2–8	Dyn A3–8	Dyn A4–8
Dyn A2–8	1					100	12	48
Dyn A3–8	1						100	73

* Dyn A3–12 and Dyn A2–12 coeluted since HPLC system I was employed for Dyn A2–13, Dyn A3–12 amounts were assumed to be negligible. Dyn A1–10, A2–10, A2–8 and A3–8 are Dyn A1–13 metabolites detected in this study. All contribute to the Dyn A4–8 pool.

Table V. Evaluation of the Contribution of a Specific Enzymatic System to the Overall Metabolism of a Dynorphin Fragment Assessed by Enzyme Inhibition (cp. Methods). Note the Difference in the Values for Aminopeptidase Inhibitors Bestatin and Leucinethiol

Inhibitor (sensitive enzyme)	Fraction of metabolism inhibited (in % calculated as F_{Enzlnh}*)				
	Dyn A1–13	Dyn A1–12	Dyn A2–12	Dyn A3–12	Dyn A4–12
GEMSA (Carboxypeptidase)	82 (Dyn A2–13)	N.T.	N.T.	N.T.	N.T.
Captopril (ACE)	N.T.	19 (Dyn A2–12)	33 (Dyn A4–12)	34 (Dyn A4–12)	46 (Dyn A5–12?)
Bestatin ("Aminopeptidase")	30 (Dyn A1–12)	88 (Dyn A1–10)	81 (Dyn A2–10)	82 (Dyn A3–10?)	76
Leucinethiol (Aminopeptidase)	0 (Dyn A1–12)	83 (Dyn A1–10)	37 (Dyn A4–12)	N.T.	59
Thiorphan (Enkephalinase A)	N.T.	0 (Dyn A2–12)	28	N.T.	N.T.

* Main metabolite observed under enzyme inhibition in parenthesis.
N.T. = not tested; 0 = no effect.

The C-terminal metabolism of Dyn A2-12 was captopril sensitive (Table V) indicating ACE activity. The resulting Dyn A2-10 was converted into Dyn A4-8 via aminopeptidases and ACE. Most of Dyn A4-12 enters the Dyn A5-12 pool (Table V). The only metabolite of Dyn A4-12 detected by HPLC was, however, Dyn A4-8 (F_{AUC} = 23%, Table IV). As the overall formation of Dyn A4-8 out of Dyn A1-13 was 33%, compared to 23% out of Dyn A4-12 (Table IV), the presence of a at least one additional pathway, presumably through Dyn A2-10 is indicated.

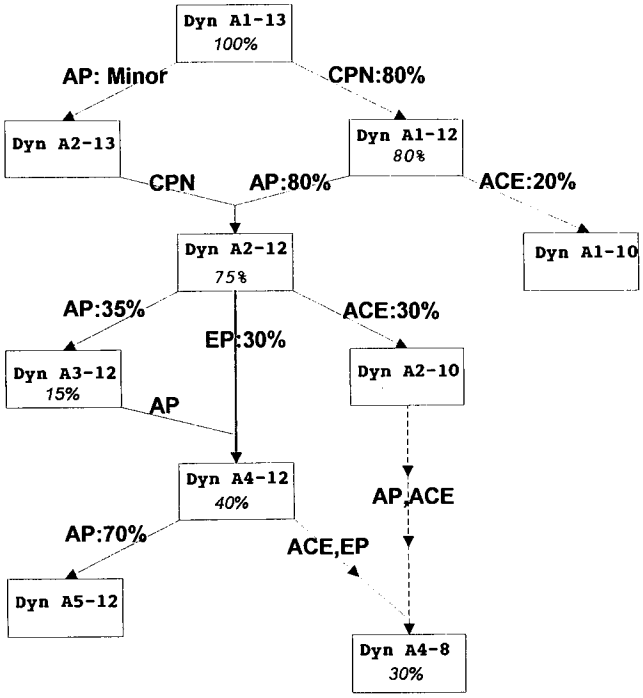

Fig. 4. Plasma metabolism of Dyn A1-13. The figures above the arrows describe the fraction of the overall metabolism suppressed by specific inhibition of the involved enzyme (F_{Enzlnh}). The percentage inside the boxes describe the conversion based on noncompartimental kinetic analysis (F_{AUC}). AP = Aminopeptidase, ACE = Angiotensin converting enzyme, CPN = Carboxypeptidase N, EP = Endopeptidase.

In summary, enzyme inhibition studies in conjunction with traditional pharmacokinetic tools, allowed the detailed assessment of the complex fate of Dyn A1-13 and its metabolites in plasma up to the fifth metabolite generation. The developed strategies seem generally applicable for detailed studies of peptide metabolism in vitro.

ACKNOWLEDGMENTS

We thank Dr. Laszlo Prokai (Center for Drug Discovery, UF) for his help by performing the MS and Dr. Emil Lin (Drug Studies Unit, UCSF) for the blocking solution. This study was supported in part by Neurobiological Technologies Incorporated, Richmond, CA.

REFERENCES

1. A. Goldstein, S. Tachibana, L.I. Lowney, M. Hunkapillar, and L. Hood. Dynorphin-(1-13), an extraordinarily potent opioid peptide. *Proc. Natl. Acad. Sci. USA.* 76:6666-6670 (1979).
2. B.H. Herman and A. Goldstein. Antinociception and paralysis induced by intrathecal dynorphin A. *J. Pharm. Exp. Ther.* 232: 27-32 (1985).
3. A.E. Takemori, H.H. Loh, and N.M. Lee. Suppression by dynorphin A and (des-Tyrl)dynorphin A peptides of the expression of opiate withdrawal and tolerance in morphine-dependent mice. *J. Pharmacol. Exp. Ther.* 266:121-124 (1993).
4. H.L. Wen and W.K.K. Ho. Suppression of withdrawal symptoms by dynorphin in heroin addicts. *Eur. J. Pharmacol.* 82: 183-186 (1982).
5. F.M. Leslie and A. Goldstein. Degradation of dynorphin A1-13 by membrane-bound rat brain enzymes. *Neuropeptides.* 2:185-196 (1982).
6. J.Z. Chou, M.J. Kreek, and B.T. Chait. Matrix-assisted laser desorption mass spectrometry of biotransformation products of dynorphin A in vitro. *J. Am. Soc. Mass Spectrom.* 5:10-16 (1994).
7. M.F. Powell, T. Stewart, L. Otvos, Jr., L. Urge, F.C.A. Gaeta, A. Sette, T. Arrhenius, D. Thomson, K. Soda, and S.M. Colon. Peptide stability in drug development. II. Effect of single amino acids substitution and glycosylation on peptide reactivity in human serum. *Pharm. Res.* 10:1268-1273 (1993).
8. A.J. Kenny and N.M. Hooper. Peptidases involved in the metabolism of bioactive peptides. In J.H. Hendriksen (ed.), *Degradation of bioactive substances: Physiology and pathophysiology,* CRC Press, Inc., Boca Raton, 1991, pp. 47-79.
9. M.J. Otero, T. Iglesias, and J.A. Fuentes. Hypoalgesic action of bestatin analogues that inhibit central aminopeptidases, but not neutral endopeptidases. *Neuropeptides.* 25:175-182 (1993).